Supplementary Fig. S1

Supplementary Fig. S1. Epigenetic compound library screening to identify compounds selectively suppressing the cell viability of BAP1-defient cancer cells. Scatter plot for 22 Aurora kinase inhibitors (**a**), 16 Sirtuin inhibitors (**b**), and 15 PARP inhibitors (**c**) grouped by fold change in selectivity for BAP1 KO#1 clone over parental M14 cells. Fold change is calculated by dividing the percentage survival of parental cells by that of M14 BAP1 KO#1 cells exposed to the individual compound at 10 μM for 6 days. Each dot represents one compound from the library, and the colors represent different fold changes (black dots: <1.5, orange dots: ≥1.5 and <3 and red dots: ≥ 3).

Supplementary Fig. S2

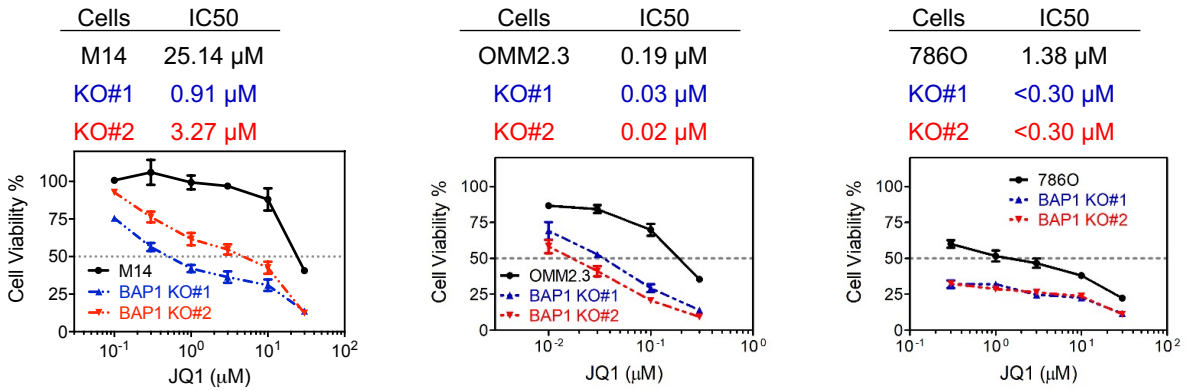

Supplementary Fig. S2. The cytotoxic effect of JQ1 on BAP1 KO cells compared to parental cells. BET inhibitor JQ1 exhibited potent and selective cytotoxicity against BAP1-deficient M14, OMM2.3 and 786O cells. Cells were treated with JQ1 at the indicated concentrations for 6 days. The data are presented as the mean ± SD (n=3) from one representative experiment out of three.

Supplementary Fig. S3

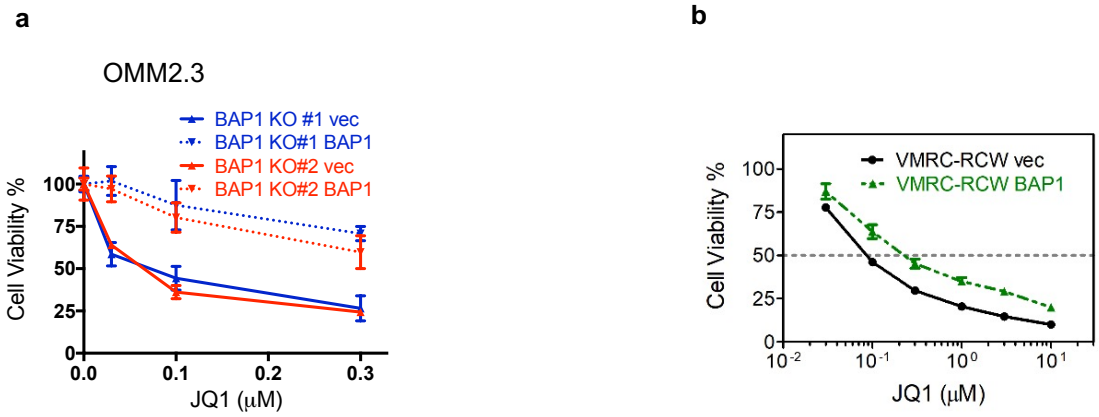

Supplementary Fig. S3. BAP1 confers resistance to BET inhibitor JQ1. (**a**) Reintroduction of BAP1 reversed the JQ1 sensitivity of OMM2.3 BAP1 KO cells. (**b**) Exogenous expression of BAP1 rendered JQ1 resistance in VMRC-RCW cells carrying *BAP1* nonsense mutation. Cells were treated with JQ1 at the indicated concentrations for 6 days. The data are presented as mean ± SD (n=3) from one representative experiment out of three.

Supplementary Fig. S4

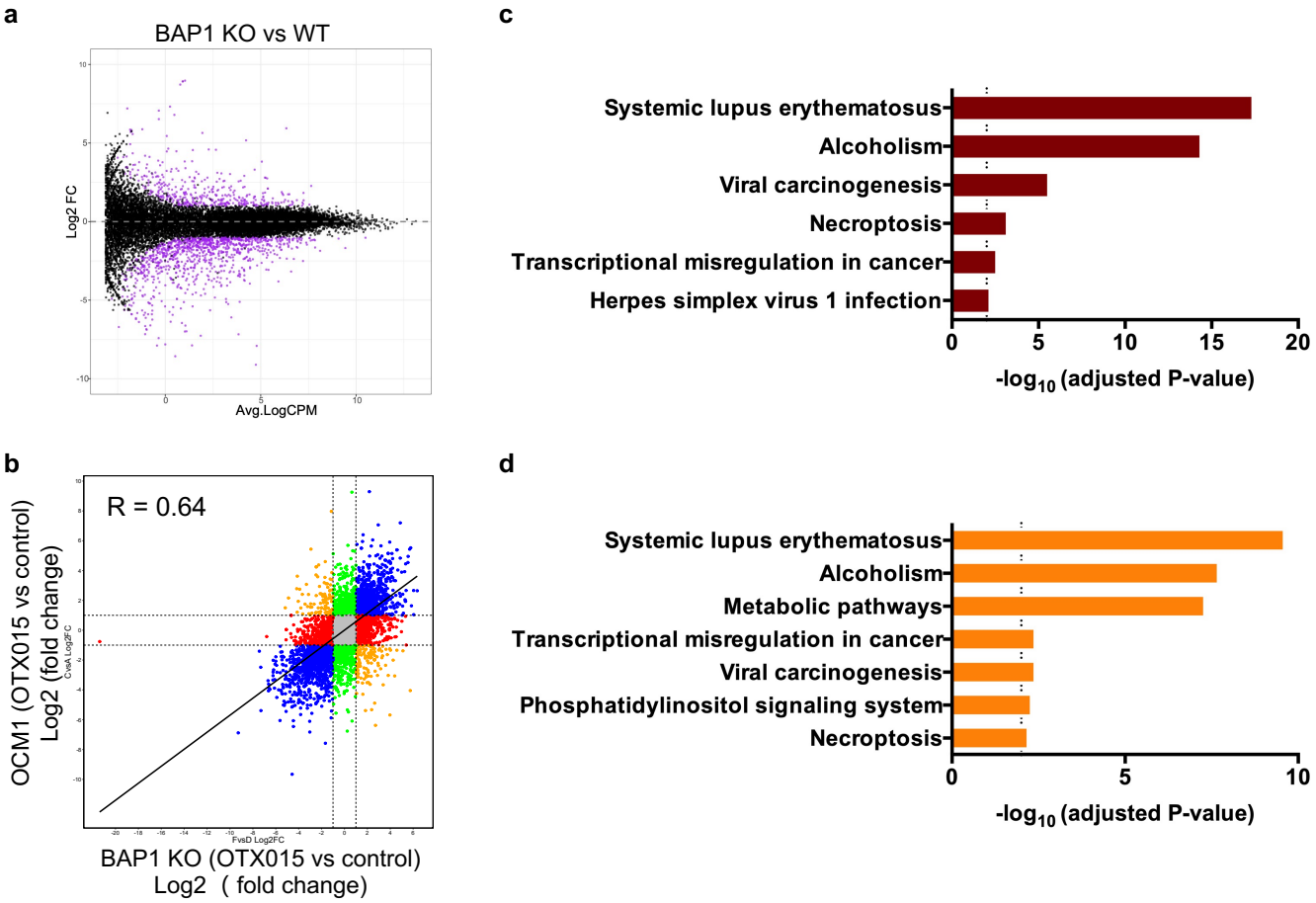

Supplementary Fig. S4. Transcriptional alterations in response to BAP1 deletion with or without OTX015 treatment. (**a**) Scatter plot showing log2 fold-change (logFC) expression between parental and M14 BAP1 KO#1 cells versus average log2 counts per million (logCPM). Differentially expressed genes (DEGs) in M14 BAP1 KO#1 cells are highlighted in purple. (**b**) Comparison of the transcriptional changes induced by OTX015 (5 μM, 24 h) in M14 BAP1 KO#1 versus parental cells. Blue dots indicate genes that are either up or down in both comparisons, orange dots are genes that are significantly up in one comparison and down in the other comparison. Green dots are genes significantly changed only in M14 cells, while red dots are genes significantly changed in M14 BAP1 KO#1 cells. R-value was calculated for the correlation; Pearson's correlation coefficient. KEGG pathways enrichment analysis for the upregulated DEGs in M14 cells (**c**) or M14 BAP1 KO#1 cells (**d**) upon 24 h OTX015 treatment at concentration of 5 μM. Pathways (adjusted P-value < 0.01) are shown.

Supplementary Fig. S5

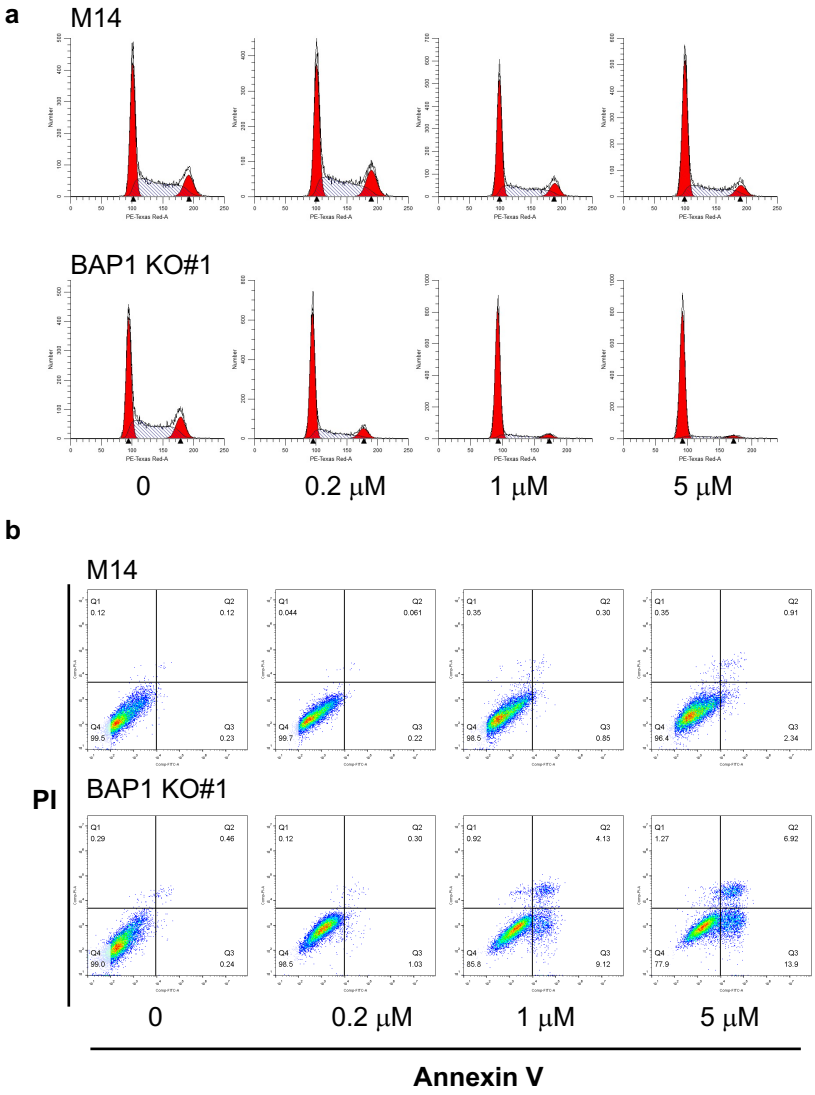

Supplementary Fig. S5. BAP1 deletion renders M14 cells more vulnerable to OTX015-induced cell cycle arrest and apoptosis. (**a**) DNA histogram showing the accumulation of G1/G0 phase cells induced by OTX015. Parental M14 or BAP1 KO#1 cells were exposed to the indicated concentrations of OTX015 for 48 h, and their DNA contents were determined by flow cytometry analysis. (**b**) Parental M14 or BAP1 KO#1 cells were exposed to the indicated concentrations of OTX015 for 96 h. Apoptosis was determined by flow cytometry after Annexin V-FITC and PI staining. Data derive from one representative experiment out of three.

Supplementary Fig. S6

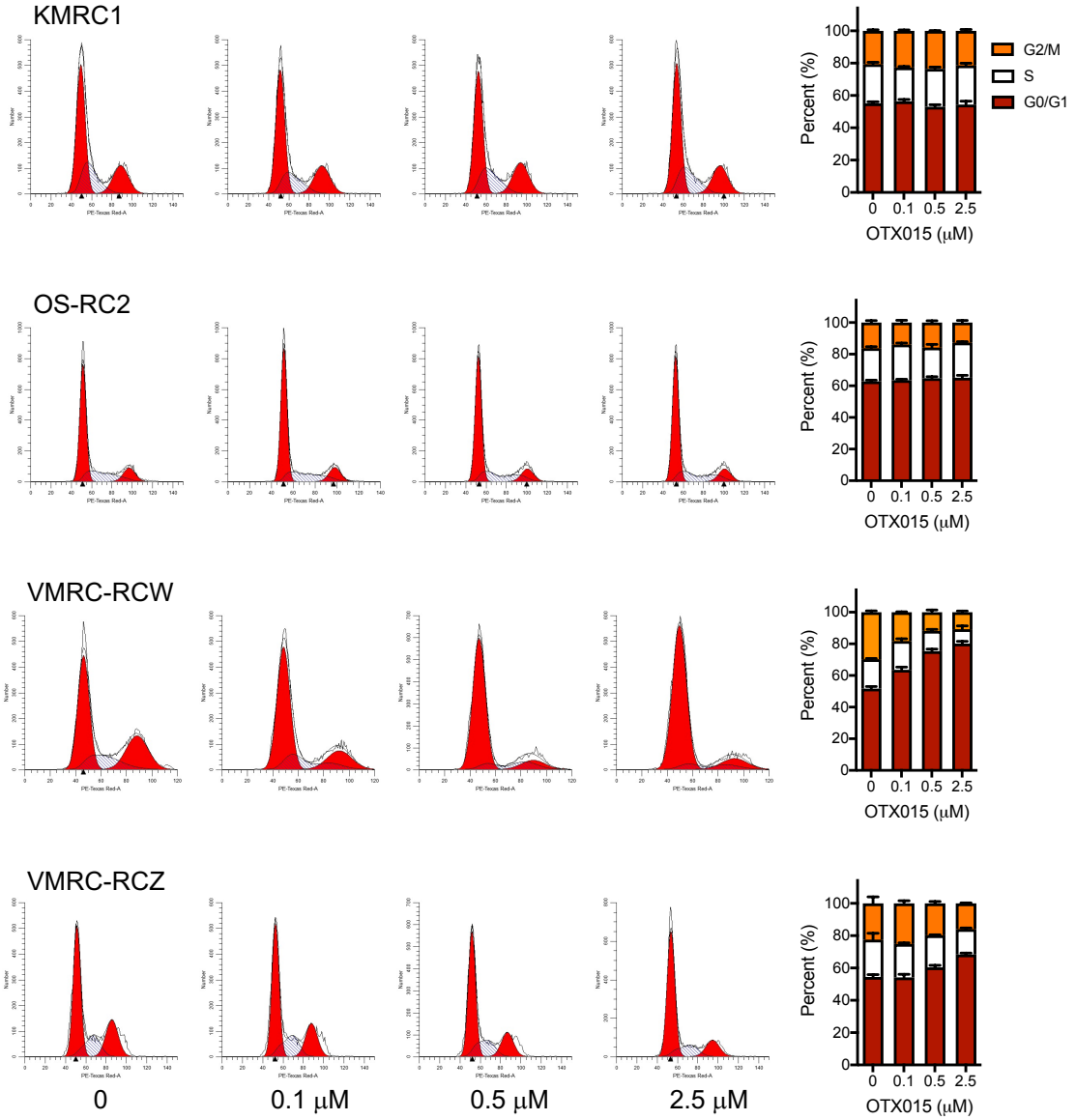

Supplementary Fig. S6. OTX015 induces G1/G0 phase arrest in BAP1-deficient ccRCC cells but not in BAP1-proficient ccRCC cells. DNA histogram showing the accumulation of G1/G0 phase cells induced by OTX015 in BAP1-deficient VMRC-RCW and VMRC-RCZ cells but not in BAP1-proficient KMRC1 and OS-RC2 cells. Cells were exposed to the indicated concentrations of OTX015 for 48 h, and their DNA contents were determined by flow cytometry analysis. Data derive from one representative experiment out of three.

Supplementary Fig. S7

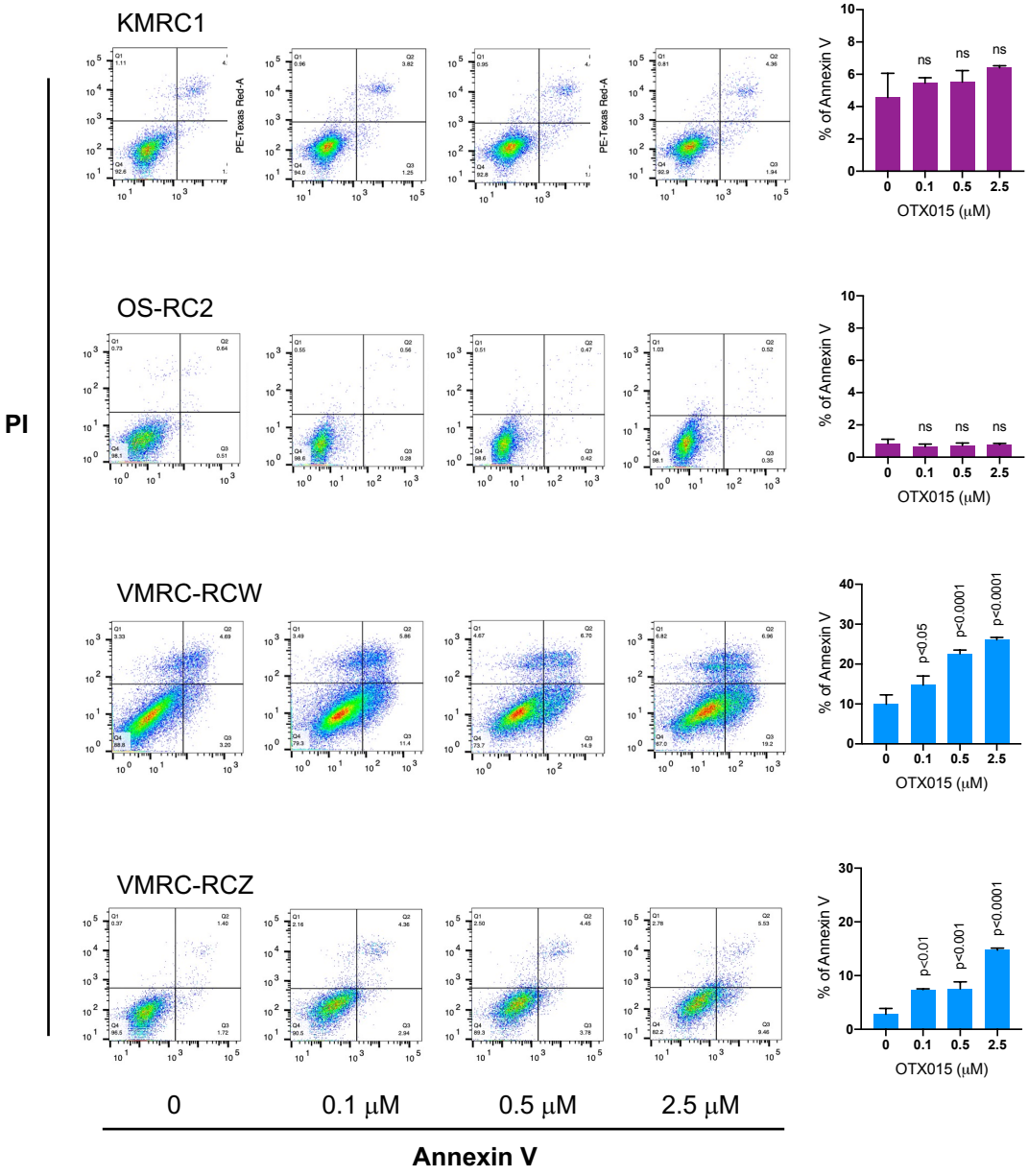

Supplementary Fig. S7. OTX015 induces apoptosis in BAP1-deficient ccRCC cells but not in BAP1-proficient ccRCC cells. BAP1-proficient cells (KMRC1 and OS-RC2) and BAP1-deficient cells (VMRC-RCW and VMRC-RCZ) were exposed to the indicated concentrations of OTX015 for 96 h. Apoptosis was determined by flow cytometry after Annexin V-FITC and PI staining. Data derive from one representative experiment out of three.

Supplementary Fig. S8

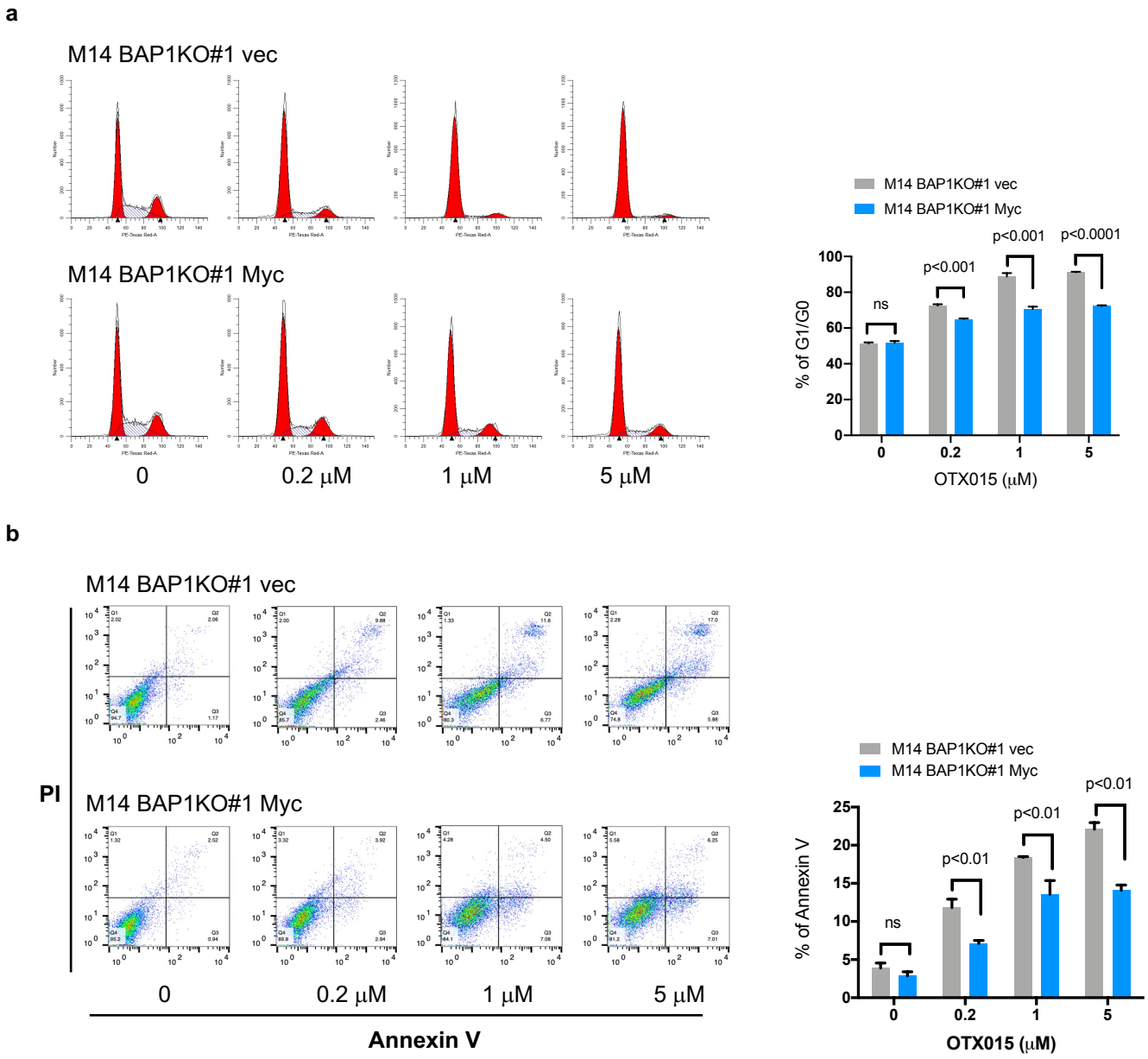

Supplementary Fig. S8. Ectopic expression of Myc attenuates G1/G0 phase arrest and apoptosis in M14 BAP1 KO#1 cells. M14 BAP1 KO#1 cells were stably transduced with control (pQCXIH-vec) or Myc (pQCXIH-HA-Myc) retroviruses. (**a**) Cells were treated with OTX015 at the indicated concentrations for 48 h, and their DNA contents were determined by flow cytometry analysis. The data are presented as mean ± SD (n=3) from one representative experiment out of three. Student's t test was used. (**b**) Cells were treated with OTX015 at the indicated concentrations for 96 h. Apoptosis was determined by flow cytometry after Annexin V-FITC and PI staining. The data are presented as mean ± SD (n=3) from one representative experiment out of three. Student's t test was used.

Supplementary Fig. S9

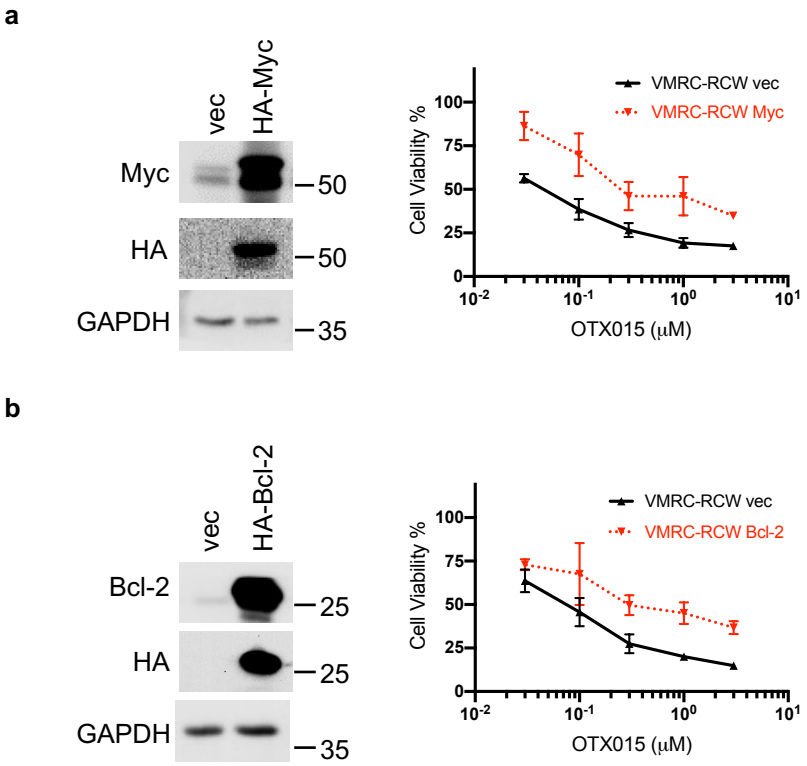

Supplementary Fig. S9. Ectopic expression of Myc protects BAP1-deficient VMRC-RCW cells from OTX015 inhibition. VMRC-RCW cells were stably transduced with control (pQCXIH-vec), Myc (pQCXIH-HA-Myc) (**a**) or Bcl-2 (pQCXIH-HA-Bcl-2) (**b**) retroviruses. Cells were then treated with OTX015 at the indicated concentrations for 6 days. The data are presented as mean ± SD (n=3) from one representative experiment out of three.

Supplementary Fig. S10

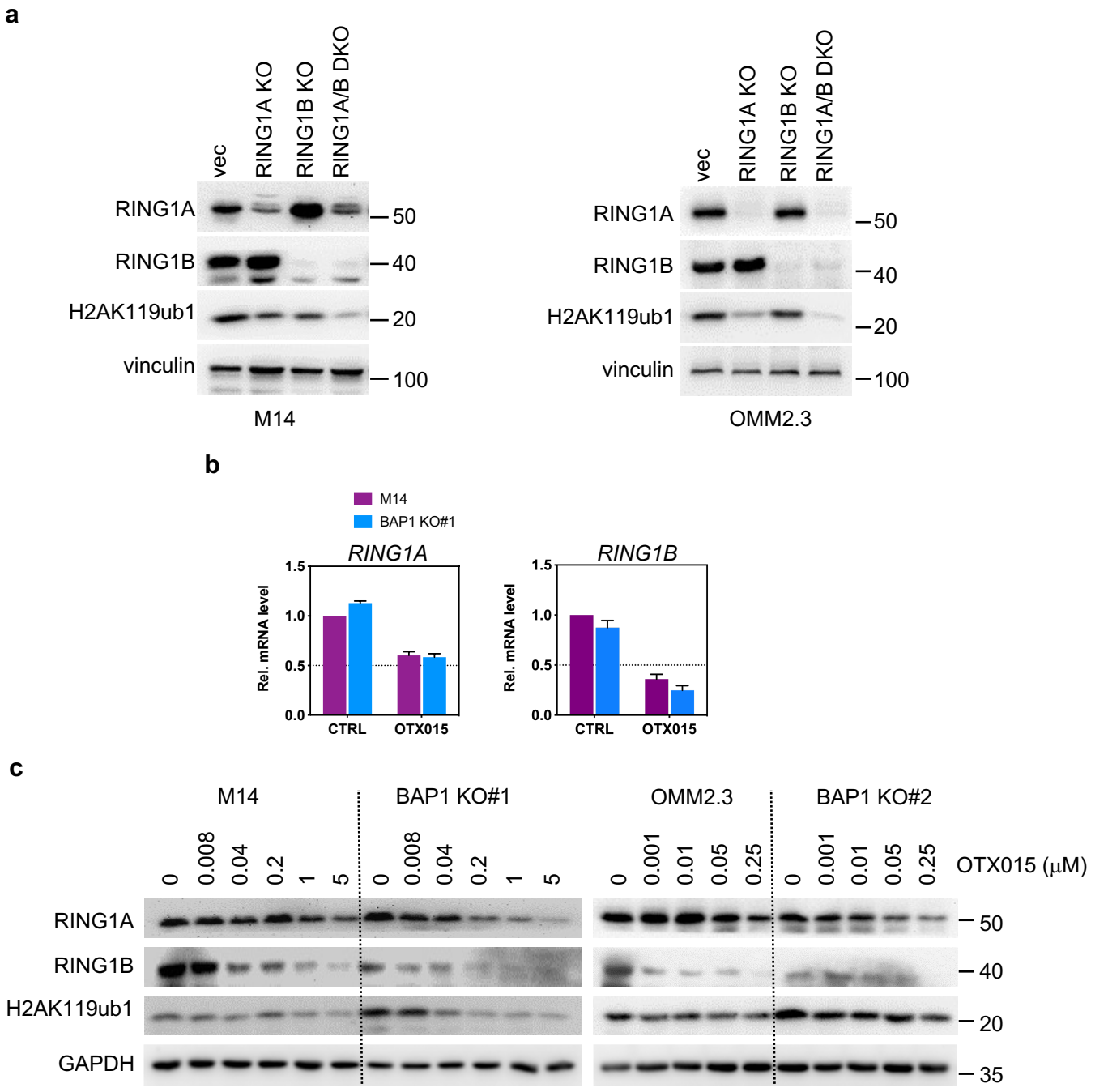

Supplementary Fig. S10. OTX015 decreases the protein levels of RING1A, RIANG1B, and H2AK119ub1. (**a**) Immunoblot analysis showing decreased H2AK119ub1 expression by RING1A or RING1B deletion by CRISPR/Cas9 in M14 (left panel) and OMM2.3 cells (right panel). (**b**) Parental and BAP1 KO#1 M14 cells were treated with OTX015 (5 μM) for 24 h. Expression levels of *RING1A* and *RING1B* were determined by qRT-PCR. Expression was normalized to *GAPDH* expression. The data are presented as mean ± SD (n=3) from one representative experiment out of three. (**c**) Immunoblot analysis was performed to measure the indicated protein expression upon 48 h OTX015 treatment at the indicated concentrations in BAP1 KO clones and their isogenic parental cells.

Supplementary Fig. S11

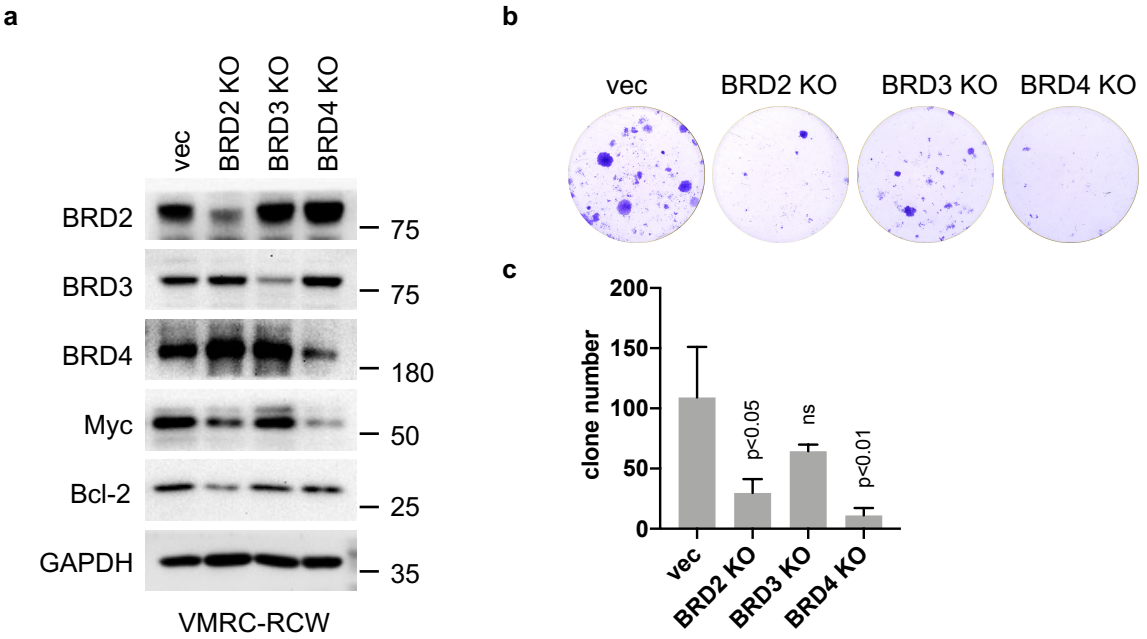

Supplementary Fig. S11. Deletion of BRD2 or BRD4 reduces colony formation in VMRC-RCW cells. (**a**) Immunoblot analysis showing the specific deletion of BRD2, BRD3 or BRD4 by CRISPR/Cas9 in VMRC-RCW cells. Images (**b**) and corresponding quantification of colony formation assays (**c**) assessing the effects of BRD2/3/4 deletion on the colony formation of VMRC-RCW cells. The data are presented as mean ± SD (n=3) from one representative experiment out of three. One-way ANOVA test was used.

Supplementary Fig. S12

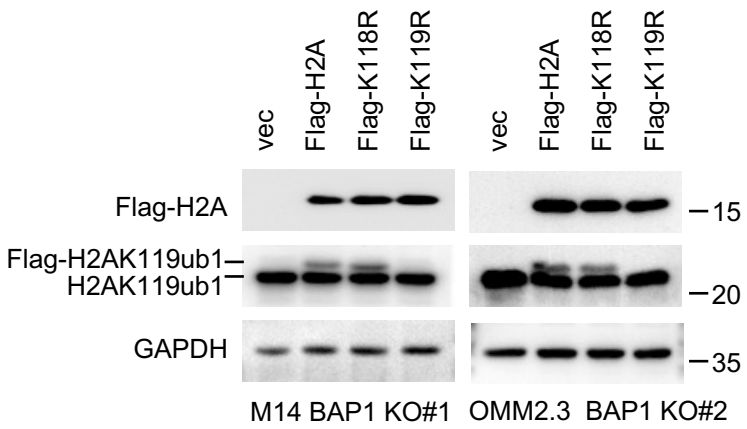

Supplementary Fig. S12. Ectopic expression of wild-type and mutant H2A (K118R and K119R). M14 BAP1 KO#1 and OMM2.3 BAP1 KO#2 cells were stably transduced with control (pQCXIH-vec), wild-type H2A (pQCXIH-Flag-H2A), H2AK118R (pQCXIH-Flag-H2AK118R), or H2AK119R (pQCXIH-Flag-H2AK119R). Immunoblot analysis showing the exogenous expression of Flag-H2A , ubiquitination of endogenous H2A (H2AK119ub1), and ubiquitination of exogenous H2A (Flag-H2AK119ub1). Unlike wild-type H2A or H2AK118R, H2AK119R can not be ubiquitinated at Arg119.

Supplementary Fig. S13

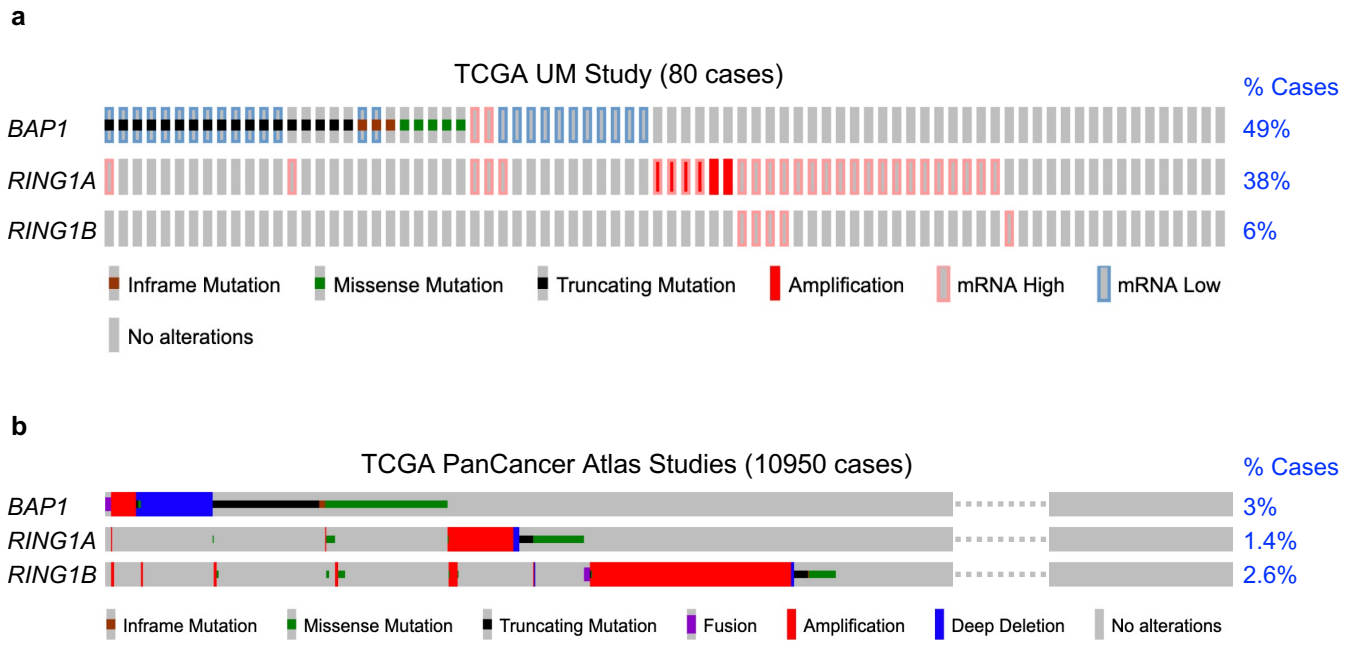

Supplementary Fig. S13. Mutation analysis of *BAP1*, *RING1A*, and *RING1B* using TCGA data. (**a**) Oncoprint depicing genetic alterations of *BAP1*, *RING1A* and *RING1B* of TCGA UM cohort downloaded from cbioportal (www.cbioportal.org). Each bar represents one sample and their respective gene mutation or expression status. P values for mutual exclusivity of the paired gene alterations were derived from one-sided Fisher Exact Test. (**b**) Oncoprint depicing genetic alterations of *BAP1*, *RING1A* and *RING1B* of TCGA PanCancer Atlas Studies downloaded from cbioportal (www.cbioportal.org). The profiled 10950 cases are from 32 studies.